ACS OMEGA

Open Access

http://pubs.acs.org/journal/acsodf

Article

Dipeptide–Copper Hybrid Nanoparticles as Efficient Laccase Mimics for Determination and Degradation of Phenolic Pollutants and Epinephrine

Lisha Feng, Kejing Mao, Xinyu Zhu, Yuyuan Chen, Jianbin Ye, Yongfang Zheng,* and Hu Zhu*

Cite This: *ACS Omega* 2025, 10, 15553−15562

Read Online

ACCESS | Metrics & More | Article Recommendations | Supporting Information

ABSTRACT: The broad application of laccase mimics is notably constrained by their costly and intricate synthesis routes. For example, researchers often use peptides to coordinate with copper ions to mimic the active sites of laccases, thereby constructing laccase mimics. However, these synthetic methods are quite complex, such as requiring high temperatures, the use of organic solvents, long durations, and cumbersome procedures. In this study, we introduce a straightforward yet highly active, robust, and versatile laccase mimic known as HH-Cu, which was synthesized through a simple precipitation reaction by combining the dipeptide HH with Cu^{2+} ions in phosphate-buffered saline (PBS). By adjusting the ratio of HH to copper ions, we were able to produce the most effective organic−inorganic hybrid nanoparticles, namely, HH-Cu, which outperforms the HH-Cu nanoflowers. HH-Cu demonstrates extraordinary catalytic efficiency, with a 4.7-fold higher maximum velocity (v_{max}) and a lower Michaelis constant (K_m) compared to natural laccase. This nanozyme is also remarkably resilient under harsh conditions such as extreme pH levels, high temperatures, and high salinity, and it shows excellent storage stability and reusability. We successfully applied this nanozyme for the degradation and quantitative detection of various phenolic pollutants and epinephrine. HH-Cu demonstrates a markedly superior sensitivity for detecting epinephrine than laccase and offers a comparable limit of detection and a broader linear range compared to other laccase mimics. This research should lay the groundwork for ongoing efforts in the development of organic−inorganic hybrid nanozymes and provide an effective method for the simple and efficient synthesis of laccase mimics.

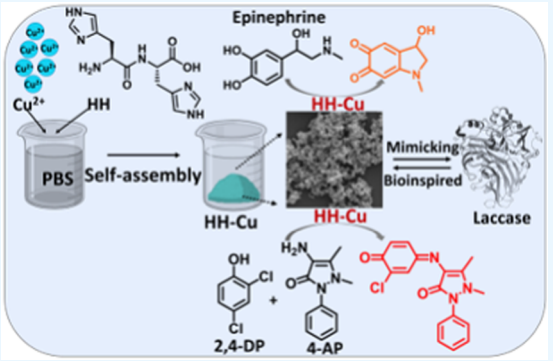

1. INTRODUCTION

Phenolic compounds are extensively utilized in various industries such as petrochemicals, food, chemicals, papermaking, wood processing, and textiles. However, their overuse and low biodegradability lead to their accumulation in soil, water, and aquatic life, posing grave threats to human health due to their potential for carcinogenic effects, neurotoxicity, reproductive toxicity, and endocrine disruption. Certain phenolic compounds like epinephrine, vital neurotransmitters of the catecholamine family, can trigger chronic diseases such as Parkinson's disease, Alzheimer's disease, and schizophrenia if their concentrations deviate from the norm.[1−4] Therefore, the detection and degradation of phenolic substances have gained widespread attention in the fields of environmental monitoring, food safety, and disease diagnosis.[5−8] It is thus urgent to develop rapid, simple, and cost-effective methods for the efficient determination and elimination of phenolic compounds. Diverse analytical methods including electroanalysis, chromatography, fluorometric analysis, and colorimetric analysis have been developed for detecting phenolic compounds.[9,10] Among these methods, the colorimetric approach has gained considerable interest owing to its simplicity, cost-effectiveness, and visual detection capabilities.[11,12]

Laccases, a class of oxidases containing multiple copper ions, can catalyze the oxidation of various organic substrates, including phenolic compounds and aromatic amines. Furthermore, laccases stand out as "green catalysts" due to their ability to directly convert dioxygen molecules into water without generating hydrogen peroxide (H_2O_2). Laccases are thus widely used for the catalytic degradation and detection of phenolic compounds.[13] Nonetheless, laccases exhibit inherent protein fragility, rendering them nonrecyclable and prone to deactivation in complex environments. Additionally, laccase production relies on fermentation, which is a tedious, time-consuming, and expensive process. These limitations substantially hinder the practical applications of laccases.

Received: January 21, 2025
Revised: February 21, 2025
Accepted: February 27, 2025
Published: April 14, 2025

Scheme 1. Schematic Illustration of the Preparation of Laccase-Mimicking HH-Cu and Its Applications

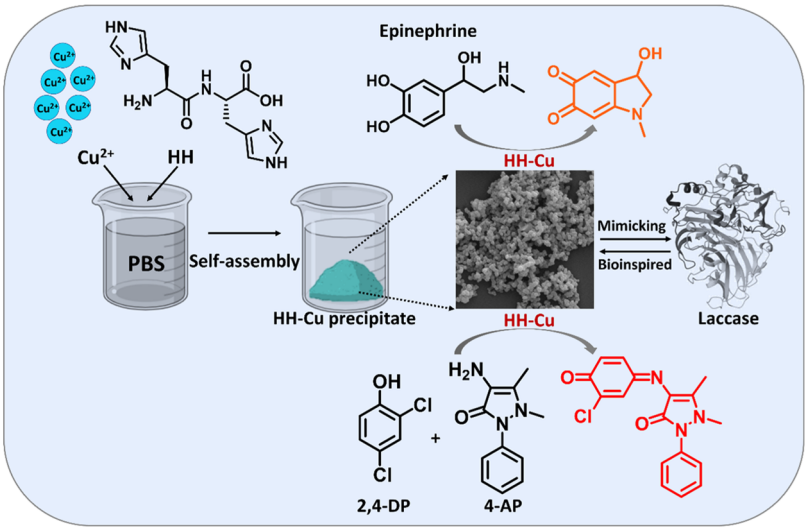

To surmount these limitations, developing nanozymes capable of mimicking laccase activities has emerged as a promising strategy. Nanozymes, characterized as nanomaterials with enzyme-like traits, hold advantages over natural enzymes such as robustness, stability under harsh conditions, recyclability, ease of long-term storage, and scalable production.[14,15] Over the past few decades, nanozymes have been considered as ideal alternatives to natural enzymes and have found widespread applications spanning biosensors, biomedicine, antibacterial agents, and environmental remediation.[16,17] Given that laccase contains four copper sites crucial to its catalytic process, most laccase-mimicking nanozymes incorporate copper elements.[18,19] For instance, nucleotide,[20−22] dipeptide cysteine−histidine,[6,23] glutathione (GSH),[24] and 2-methylimidazole[7] have been used to coordinate with copper to construct laccase-mimicking nanozymes. Moreover, some copper-free nanomaterials have exhibited laccase-mimicking activity.[8,25−28] Yet, the repertoire of existing nanomaterials demonstrating laccase-mimicking activity remains limited. Further, many laccase-mimicking nanozymes are extremely complex, unstable at high temperature, and susceptible to salts and pH.[25,26,29] The synthesis methods for many laccase-mimicking nanozymes are intricate and not environmentally friendly. Further efforts are thus needed to develop laccase-mimicking nanozymes with superior activities and durability through simplified methodologies.

Organic−inorganic hybrid flower-shaped nanomaterials, also known as nanoflowers, entail the assembly of hierarchical nanosheets comprising both organic and inorganic constituents. This class of hybrid nanomaterials was initially unveiled in 2012 when Ge et al. demonstrated the formation of nanoflower precipitates through the mixing and stirring of protein BSA with copper sulfate in phosphate buffer saline (PBS).[30] Subsequently, this kind of organic−inorganic hybrid nanoflowers has gained widespread attention.[31] The inorganic component of nanoflowers typically consists of transition metal phosphates, while the organic counterpart encompasses enzymes and proteins. Organic−inorganic hybrid nanoflowers can be easily synthesized under mild conditions, by making use of the coordination between biomolecules and inorganic ions, including Ca^{2+}, Cu^{2+}, Zn^{2+}, Mn^{2+}, Co^{2+}, and Fe^{2+}.[32−35] These nanoflowers have garnered substantial interest due to their ability to retain high activity and exceptional stability of encapsulated organic components within hierarchically organized flower matrices.[31] At present, this methodology chiefly serves enzyme immobilization to enhance the stability. Numerous enzymes have been reported to adopt nanoflower structures with copper ions in PBS, significantly enhancing their activity and stability.[35−38] It is currently rare to construct nanozymes by using such a simple and quick method, with some examples reported for peroxidases.[39,40] Its potential for constructing laccase mimics remains largely unexplored.

In this work, we synthesized various laccase-mimicking nanozymes by simply mixing different dipeptides or amino acids with copper ions in PBS. Among them, the dipeptide HH exhibited the highest activity. By modulating the ratio of HH to copper ions, we obtained the best-performing dipeptide−copper hybrid nanoparticles (HH-Cu), which is superior to the HH-Cu nanoflower. Compared to natural laccase, our reported laccase mimic HH-Cu showed 4.7 times higher v_{max} and a lower K_m when employing 2,4-DP as a substrate. Furthermore, HH-Cu demonstrated remarkable stability under extremely harsh conditions, excellent storage stability, and recyclability. We successfully used this nanozyme for the degradation and quantitative detection of diverse phenolic pollutants and epinephrine (Scheme 1).

2. MATERIALS AND METHODS

2.1. Materials. Peptides and amino acids (histidine-histidine (HH), phenylalanine-histidine (FH), phenylalanine-tryptophan (FW), cysteine−histidine (CH), histidine (H), cysteine (C), and phenylalanine (F)) were purchased from Bankpeptide Biological Technology Co., Ltd. Laccase (≥0.5 U/mg) was purchased from Yuanye Biotechnology Co., Ltd. (Shanghai, China). PBS buffer (pH 7.4) was obtained from Sangon Biotech (Shanghai) Co., Ltd. 2,4-dichlorophenol (2,4-DP), 4-aminopyridine (4-AP), phenol, chlorophenol, naphthol, epinephrine, 2-(N-morpholino) ethanesulfonic acid (MES), horseradish peroxidase (HRP), and 2,2′-azino-bis(3-ethylbenzothiazoline-6-sulfonic acid) (ABTS) were all purchased from Macklin Biochem Technology Co., Ltd. (Shanghai, China). Hydroquinone and 2-aminophenol were obtained from Adamas-Beta Reagent Co., Ltd. (Shanghai, China). Copper chloride, sodium chloride, and hydrogen peroxide

https://doi.org/10.1021/acsomega.5c00623
ACS Omega 2025, 10, 15553−15562

were purchased from Sinopharm Chemical Reagent Co., Ltd. (Shanghai, China). All materials were used without further purification.

2.2. Nanozyme Preparation. To prepare laccase-mimicking nanozymes, 5 mM dipeptides or amino acids (HH, FH, FW, CH, C, H, mixture of C and H (C+H), and F) was mixed with 5 mM copper chloride in PBS. The mixture was then heated at 90 °C for 50 min and settled overnight at room temperature. Afterward, the precipitates were collected by centrifugation at 10,000 rpm for 5 min and washed with ultrapure water three times to remove excess reactants. The obtained precipitates were then dried under vacuum conditions. To explore the impact of varying HH-to-copper chloride ratios on catalytic activity during preparation, different concentrations of HH (5, 10, and 15 mM) were mixed with 5 mM copper chloride in PBS or different concentrations of copper chloride (10 and 15 mM) were mixed with 5 mM HH in PBS to produce HH-Cu nanozyme with varying proportions (n_{HH}/n_{Cu}= 3:1, 2:1, 1:1, 1:2, and 1:3). Notably, no precipitate was obtained when n_{HH}/n_{Cu} is 3:1 and 2:1. When n_{HH}/n_{Cu} is 1:1 (HH-Cu), 1:2 (HH-2Cu), and 1:3 (HH-3Cu), precipitates were successfully obtained. The control sample formed in the absence of HH or $CuCl_2$ was designated as copper phosphate [$Cu_3(PO_4)_2$] precipitate and HH.

2.3. Characterization of HH-Cu. HH-Cu was characterized using scanning electron microscopy (SEM) (Phenomenon LE, Phenom-World, The Netherlands). X-ray photoelectron spectroscopy (XPS) data are collected using the Thermo Scientific K-Alpha XPS instrument from the United States with Al Kα X-ray source (1486.6 eV). The X-ray diffraction data were obtained on an instrument (PANalytical, The Netherlands) equipped with a Cu filter over a range of 5−80°, with a step size of 0.013° and a scanning speed of 5°/min. The infrared spectra were measured by using a Nicolet 5700 spectrometer (Thermo). All samples were scanned over a range of 4000−400 cm^{-1} at a resolution of 4 cm^{-1}.

2.4. Evaluation of Laccase-like Activity of HH-Cu. The catalytic activities of HH-Cu and laccase were evaluated through a colorimetric reaction involving 2,4-dichlorophenol (2,4-DP) and 4-aminopyridine (4-AP).[6] In brief, a solution of 2,4-DP (1 mg/mL, 100 μL) and 4-AP (1 mg/mL, 100 μL) was added to MES buffer solution (pH = 6.5, 700 μL). Subsequently, HH-Cu or laccase (0.35 mg/mL, 100 μL) was added to the mixture, and the reaction was allowed to proceed at room temperature for 1 h. After the reaction, the mixture was centrifuged (12,000 rpm, 3 min), and the absorbance of the supernatant was measured at 510 nm.

To verify that the catalytic products of the nanozyme do not contain hydrogen peroxide (H_2O_2), we first mixed a solution of 2,4-dichlorophenol (2,4-DP) (1 mg/mL, 100 μL) with MES buffer (pH = 6.5, 800 μL). Then, we added HH-Cu (0.35 mg/mL, 100 μL) to the mixture and allowed it to react at room temperature for 1 h. After the reaction, the mixture was centrifuged and the supernatant was collected. Next, we added horseradish peroxidase (HRP) and ABTS to the supernatant, followed by the addition of H_2O_2. In each step, we observed changes in the solution's color and recorded the absorbance of the supernatant at 414 nm.

2.5. Determination of Catalytic Kinetic Parameters. Different concentrations of 2,4-DP (5, 10, 20, 30, 40, 60, 80, and 100 μg/mL) were mixed separately with 0.15 mg/mL 4-AP (in excess in all reactions) and 35 μg/mL HH-Cu or laccase. The initial reaction rates were measured. The kinetic parameters (K_m and v_{max}) were calculated using the Michaelis−Menten equation:

$$1/v_0 = (K_m/v_{max}) \times (1/[S_0]) + 1/v_{max}$$

where v_0 is the apparent initial catalytic rate, K_m is the apparent Michaelis−Menten constant, v_{max} is the maximum apparent initial reaction rate, and S_0 is the initial substrate concentration.

2.6. Assessment of Catalytic Stability. The experimental procedure was adapted from a previous work.[6] For studying the effect of pH, HH-Cu or laccase was incubated at different pH (pH 3−9) for 7 h, followed by activity measurement. The catalytic activity at pH 6 is used as a reference. Additionally, the morphologies of HH-Cu after different pH treatments were characterized using SEM. To study the effect of temperature, HH-Cu and laccase were stored at temperatures ranging from −20 to 90 °C for 45 min. Then, the catalytic activity was measured with the activity at 30 °C as the reference. The morphologies of HH-Cu after different temperature incubations were also examined using SEM. Different concentrations of sodium chloride (0, 100, 200, 300, and 500 mM) are added to the reaction system to assess the influence of ionic strength on catalytic activity of HH-Cu and laccase. Different ethanol contents (0, 25, 50, 75, and 100% v/v) were mixed with the reactants to study the impact of organic solvents on the catalytic activity of HH-Cu and laccase. To evaluate the effect of storage time on catalytic activity, HH-Cu and laccase were placed at room temperature, and activity measurement was conducted at regular intervals. For assessing the recyclability of HH-Cu, a mixture of 2,4-DP (1 mg/mL, 100 μL), 4-AP (1 mg/mL, 100 μL), MES buffer (pH = 6.5, 700 μL), and HH-Cu (0.35 mg/mL, 100 μL) was prepared at room temperature. After reaction for 1 h, the precipitate was collected by centrifugation (12,000 rpm, 3 min), washed three times with ultrapure water, and reused for the next reaction cycle. The absorbance of the supernatant at 510 nm was measured. Each experimental data point was obtained from three replicates to ensure the reliability and reproducibility of the results.

2.7. Oxidation of Phenolic Pollutants Catalyzed by HH-Cu. HH-Cu nanozyme was employed for degradation and detection of phenolic pollutants such as phenol, 4-chlorophenol, hydroquinone, 2-aminophenol, 1-naphthol, and 2,4-dichlorophenol.[25] HH-Cu (0.35 mg/mL, 100 μL) and different concentrations of phenolic compounds were mixed with MES buffer (pH = 6.5). The mixtures were allowed to react at room temperature for 1 h, and after centrifugation, the absorbance of the oxidation product at its corresponding maximum wavelength was measured in the supernatant. The detection limit was calculated as 3σ/b, where σ is the standard deviation of the blank signals and b is the slope of the regression line. For some phenolic compounds that did not form colored oxidation products, such as 2,4-DP, phenol, 4-chlorophenol, and 1-naphthol, 4-AP was added, and wine-red colored products were formed with absorption maxima at 510 nm. Each experimental data point was obtained from three replicates to ensure the reliability and reproducibility of the results.

2.8. Oxidation of Epinephrine Catalyzed by HH-Cu. HH-Cu or laccase (0.35 mg/mL, 100 μL) was mixed with different concentrations (0.05, 0.1, 0.2, 0.4, 0.8, 1, 2, 4, 6, 8, 12, and 14 mM) of epinephrine (50 μL) and MES buffer (pH = 6.5 and 850 μL). The mixtures were allowed to react at room temperature for 1 h. After centrifugation (12,000 rpm, 3 min), the absorbance of the supernatants at 485 nm was measured.

https://doi.org/10.1021/acsomega.5c00623
ACS Omega 2025, 10, 15553−15562

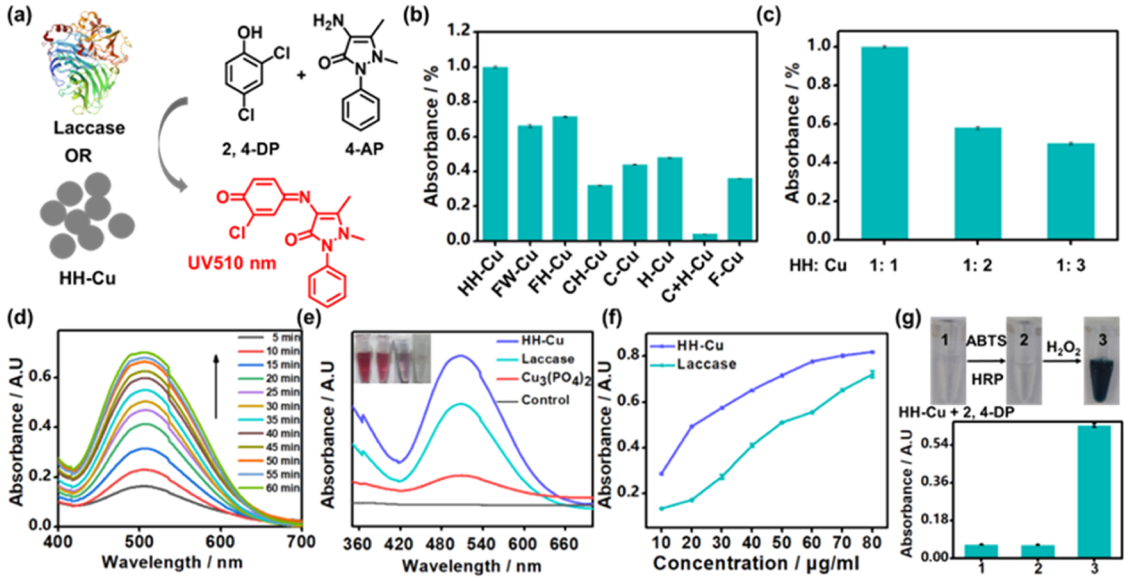

Figure 1. (a) Reaction of 2,4-DP and 4-AP catalyzed by laccase or HH-Cu. (b) Comparison of the laccase-like activity of the hybrid nanomaterials (HH-Cu, FW-Cu, FH-Cu, CH-Cu, C-Cu, H-Cu, C+H-Cu, and F-Cu). (c) Comparison of the catalytical activity of the laccase mimics with different ratios of HH and Cu^{2+} in the preparation process. (d) The changes of UV−vis spectrum of the 2,4-DP/4-AP system catalyzed by HH-Cu. (e) Comparison of the laccase-like activity of HH-Cu with laccase at the same mass concentration. (f) Comparison of the laccase-like activity of HH-Cu with laccase at different concentrations. (g) Photographs of HH-Cu and 2,4-DP reaction in MES buffer (1) and after centrifugation, upon the addition of ABTS and HRP to the supernatant collected (2), and after adding hydrogen peroxide to the supernatant (3). The histogram at the bottom corresponds to the absorption intensity at 414 nm of (1), (2), and (3).

The detection limit was calculated as $3\sigma/b$, where σ represents the standard deviation of the blank signal and b represents the slope of the regression line. Each experimental data point was obtained from three replicates to ensure the reliability and reproducibility of the results.

3. RESULTS AND DISCUSSION

3.1. Screening Laccase Mimic with High Catalytic Activity and Its Characterization. Laccases are characterized by four distinct copper sites: Type 1 (T1), Type 2 (T2), and binuclear Type 3 (T3) Cu sites. Oxidation of substrates occurs at the T1 Cu site, with electrons transferring from the T1 Cu site to the trinuclear Cu cluster (T2/T3) where molecular oxygen transforms into water through a cysteine−histidine (Cys−His) pathway. To replicate the active sites of laccases, a selection of dipeptide and amino acid precursors, including HH, FW, FH, CH, C, H, F, and a blend of C and H, were utilized in the synthesis of laccase mimics. These precursors were mixed with copper chloride in PBS, resulting in a precipitate formation. The obtained precipitates were washed with ultrapure water and then dried under a vacuum. Through this simple method, we obtained various laccase mimics (HH-Cu, FW-Cu, FH-Cu, CH-Cu, C-Cu, H-Cu, C+H-Cu, and F-Cu). The laccase-like catalytic activity of these mimics was assessed through a representative chromogenic reaction involving 2,4-dichlorophenol (2,4-DP) and 4-aminopyridine (4-AP). The individual 2,4-DP and 4-AP do not have absorbance at 510 nm. However, 2,4-DP, which is the true substrate, undergoes redox reactions catalyzed by laccase or laccase mimics. The oxidation product then reacts with 4-AP to generate a wine-red product with maximum absorption at 510 nm (Figure 1a). HH-Cu demonstrated a superior performance among these laccase mimics. The investigation proceeded by varying the proportions of HH to copper chloride ($CuCl_2$) in the synthesis, with ratios tested at 3:1, 2:1, 1:1, 1:2, and 1:3 (n_{HH}/n_{Cu}). Successful precipitation occurred at ratios of 1:1 for HH-Cu, 1:2 for HH-2Cu, and 1:3 for HH-3Cu, with no precipitate formation observed at the 3:1 and 2:1 ratios. As depicted in Figure 1c, HH-Cu exhibited the most potent catalytic activity. Consequently, HH-Cu was selected for subsequent experiments. Cu^{2+} can also slowly catalyze the reaction between 2,4-DP and 4-AP, causing the reaction solution to turn light pink color. To eliminate the interference of free Cu^{2+} in the solution, we conducted relevant experiments, and the data indicate that the laccase activity in the supernatant is very weak, whereas the activity in the precipitate is very strong, which rules out the interference of free copper ions (Figure S1). The comparative catalytic efficiency of HH-Cu and laccase was assessed using a colorimetric assay with 2,4-DP and 4-AP. Throughout the reaction, there was a consistent rise in absorbance at 510 nm within the HH-Cu catalyzed system, as shown in Figure 1d. At equivalent mass concentrations, HH-Cu significantly outperformed laccase in terms of catalytic activity, as illustrated in Figure 1e,f. Unlike certain oxidases that produce hydrogen peroxide (H_2O_2) as an intermediate, laccase catalyzes the direct reduction of oxygen to water, bypassing the generation of H_2O_2. To confirm the absence of H_2O_2 in the oxygen reduction process catalyzed by HH-Cu, a mixture of 2,4-DP and HH-Cu was prepared without the addition of 4-AP to avoid any color interference. After allowing for a complete reaction, the supernatant was obtained by centrifugation at 10,000 rpm for 5 min. When horseradish peroxidase (HRP) and ABTS were added to this supernatant, there was no color change or absorbance detected at 414 nm, indicating no production of H_2O_2. The addition of H_2O_2 to the mixture resulted in an immediate green color change, further confirming that no H_2O_2 was generated during the catalytic reaction by HH-Cu. In conclusion, HH-Cu has been identified as a nanozyme with activity akin to that of laccase.

https://doi.org/10.1021/acsomega.5c00623
ACS Omega 2025, 10, 15553−15562

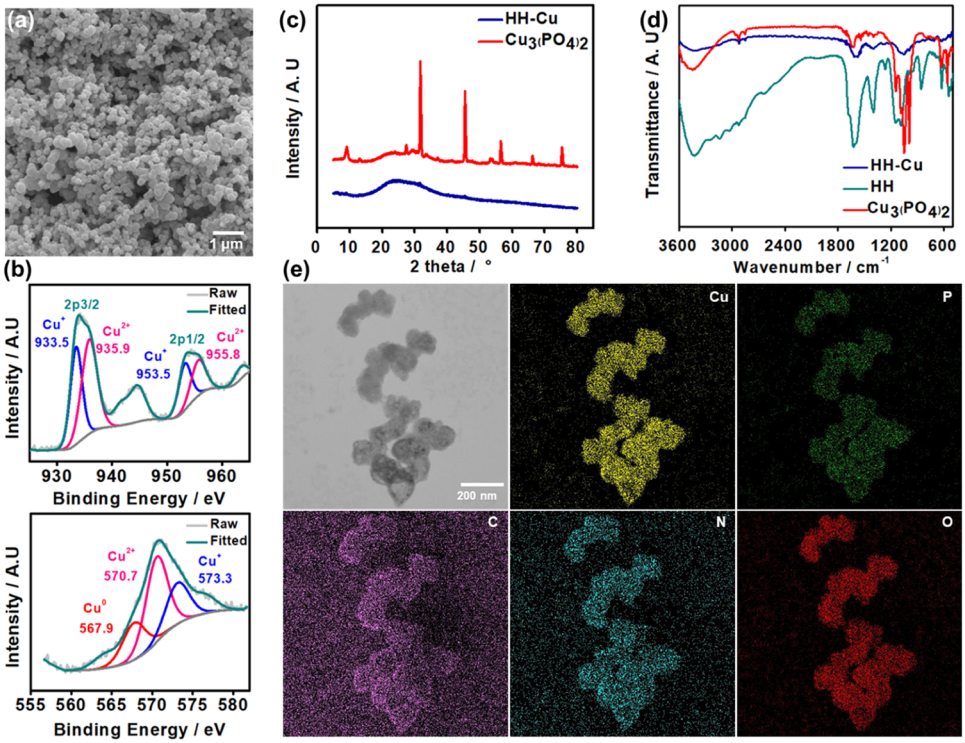

Figure 2. (a) SEM image of HH-Cu. (b) Cu 2p XPS spectrum of HH-Cu. (c) XRD characterization of HH-Cu. (d) FTIR spectrum of HH-Cu. (e) EDS mapping of HH-Cu.

Subsequently, the mechanisms behind the difference in catalytic activity of HH-Cu, HH-2Cu, and HH-3Cu were investigated. We characterized their morphologies using SEM. HH-Cu exhibited circular particle shape with a size of approximately 200 nm (Figure 2a), while HH-2Cu and HH-3Cu exhibited nanoflower shapes ranging from 3 to 10 μm (Figure S2), which is a common structural form for organic−inorganic hybrid nanomaterials.[30] Additionally, X-ray photoelectron spectroscopy (XPS) was used to study the differences in the copper oxidation states between HH-Cu and HH-2Cu. The full-scan spectra (Figure S3) indicated the presence of C, N, O, P, and Cu elements in both HH-Cu and HH-2Cu, consistent with the elements of ligand HH and copper ions. The high-resolution XPS spectrum of HH-Cu (Figure 2b) showed peaks at 935.9 and 955.8 eV, corresponding to Cu $2p_{3/2}$ and Cu $2p_{1/2}$ electrons in Cu^{2+}. The lower binding energy peaks at 933.5 eV ($2p_{3/2}$) and 953.5 eV ($2p_{1/2}$) indicated the presence of Cu^{+}. Cu LMM Auger spectra revealed Cu^{+} at 573.3 eV and Cu^{2+} at 570.7 eV, along with a small amount of Cu^{0} atoms (567.9 eV). We speculate that this Cu^{0} may result from Cu^{2+}/Cu^{+} reduction by HH.[6] The XPS spectrum of HH-2Cu (Figure S4) closely resembled that of HH-Cu, differing in peak intensities. Previous results indicated that higher Cu^{+}/Cu^{2+} ratios were associated with enhanced laccase-like activity.[41] The Cu^{+}/Cu^{2+} ratios of HH-Cu and HH-2Cu were calculated to be 0.74 and 0.31, respectively. In summary, HH-Cu showed a higher catalytic activity than HH-2Cu and HH-3Cu, likely due to its morphology and higher Cu^{+} content. Additional characterization methods provided insight into HH-Cu's structure. XRD data (Figure 2c) revealed HH-Cu's noncrystalline nature, contrasting with control group $Cu_3(PO_4)_2$. Infrared spectra of HH-Cu differed significantly from those of control groups HH and $Cu_3(PO_4)_2$ (Figure 2d). TEM images aligned with SEM morphologies, while elemental mappings confirmed C, N, O, P, and Cu elements in HH-Cu (Figure 2e). Neither HH alone in PBS nor the addition of copper ions alone to PBS results in the formation of nanoparticles (Figure S5). These results indicate the involvement of HH, copper ions, and phosphate ions in HH-Cu.

Subsequently, we compared the catalytic kinetics of HH-Cu with those of laccase. Different concentrations of 2,4-DP (5, 10, 20, 30, 40, 60, 80, and 100 μg/mL) were mixed with 0.15 mg/mL 4-AP (in excess in all reactions) and 35 μg/mL HH-Cu or laccase, and the changes in absorbance at 510 nm were meticulously monitored. The kinetic parameters were calculated by using the Michaelis−Menten equation. Figure S6 and Table S1 show the v_{max} and K_m of HH-Cu (K_m: 0.142 mM, v_{max}: 1.37×10^{-3} mM min^{-1}) and laccase (K_m: 0.154 mM, v_{max}: 2.94×10^{-4} mM min^{-1}), illustrating that HH-Cu outperformed laccase, exhibiting a 4.7-fold higher v_{max} and lower K_m. This discrepancy indicated that HH-Cu boasted superior substrate affinity and reaction rate, ultimately heightening the kinetic performance. Compared to most of the reported laccase mimics, HH-Cu has comparable or smaller K_m values, indicating that our nanozyme has good substrate affinity (Table S1).

Inspired by the active sites of laccase, many researchers have constructed laccase mimics using peptides and amino acids coordinated with copper, especially the dipeptide CH. A pioneering work by He's group published in 2019 involved the synthesis of laccase mimic through the coordination of dipeptides with copper.[6] However, their synthetic method is entirely different from ours. They mixed an aqueous Cys−His dipeptide solution, an aqueous copper(II) chloride solution, and 4 mL of DMF in a 15 mL glass pressure tube at 140 °C for 4.5 h. This method requires the use of an organic solvent and a high temperature. Numerous subsequent studies on the

https://doi.org/10.1021/acsomega.5c00623
ACS Omega 2025, 10, 15553−15562

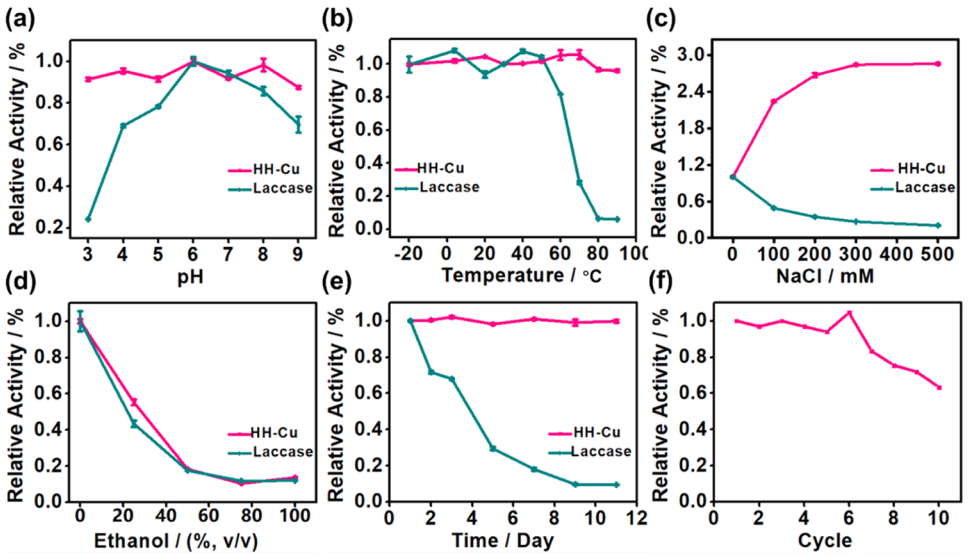

Figure 3. Comparison of the stability of HH-Cu and laccase at different pH (a), temperature (b), NaCl concentration (c), content of ethanol (d), and storage time (e). (f) Recyclability of HH-Cu.

synthesis of peptide−copper composites to mimic laccase have referenced this method[18,20] For example, the one published by Lu's group in 2022 also involve mixing the dipeptide CH with copper salts in DMF and then heating at high temperatures, which is the same as the previous methods mentioned above.[23] However, our synthesis method only requires mixing dipeptides with copper salts in PBS to obtain the product, without the need for organic solvents and high temperatures such as 120 °C. Our synthetic method requires not only the dipeptide and copper ions but also the participation of phosphate ions. The phosphate ions can quickly form a precipitate with copper ions, and the dipeptide can coordinate with the metal ions. All three components are indispensable. From the SEM images (Figure S5), it can also be observed that neither the peptides alone in PBS nor the addition of copper ions alone to PBS results in the formation of nanoparticles. The dipeptide acts like a binder that combines the phosphoric copper to form our nanoparticles HH-Cu.[31] Our method can quickly form a precipitate, so the synthesis of this nanozyme is very convenient and fast. Recently, numerous publications on laccase mimics have been published, greatly enriching the variety of laccase mimics. However, some of these methods necessitate the use of precious metals, others demand sustained heating at elevated temperatures, and some even require protection from light.[27,28,42] Overall, our method remains straightforward and simple in comparison. Our method was inspired by an article from Ge et al.in 2012, where they demonstrated the formation of nanoflower precipitates BSA-$(Cu)_3(PO_4)_2$ through the mixing and stirring of the protein BSA with copper sulfate in phosphate buffer saline (PBS).[30] However, this method has rarely been used to construct laccase mimics. Consequently, our material is fundamentally different from those reported in other literature.

3.2. Catalytic Stability and Recyclability of HH-Cu. Robust stability and reusability are crucial attributes for the practical applications of nanozymes. We compared the catalytic stability of HH-Cu and laccase under different pH, temperature, ionic strength, ethanol conditions, and storage time. Initially, HH-Cu and laccase were incubated at various pH ranging from 3.0 to 9.0 for 7 h. Morphological changes in HH-Cu were investigated through SEM analysis. It was evident that HH-Cu maintained its original morphology under different pH conditions, indicating the structural stability of HH-Cu (Figure S7). Subsequently, we measured their catalytic activities with the catalytic activity at pH 6 serving as the control. As shown in Figure 3a, catalytic activity of laccase was severely impaired by pH fluctuations, losing approximately 80% of its catalytic potency after incubation at pH 3.0, whereas the catalytic activity of HH-Cu remained nearly unaffected. Even after incubation at pH 3 or 9, HH-Cu retained over 85% of its catalytic activity.

We proceeded to scrutinize the thermal stability of laccase and HH-Cu by subjecting them to temperatures ranging from −20 to 90 °C for 45 min. SEM analysis of HH-Cu revealed its structural stability after exposure to different temperatures, indicating remarkable structural stability (Figure S8). Subsequently, we measured the catalytic activities of laccase and HH-Cu. As depicted in Figure 3b, with increasing temperature, the catalytic activity of laccase declined gradually and became completely lost at 80 °C. In contrast, the catalytic activity of HH-Cu remained nearly unscathed. This underscores the remarkable thermal stability of HH-Cu, positioning it as a favorable candidate for applications in environments with a fluctuating temperature.

We investigated the effect of the ionic strength on the catalytic activity of laccase and HH-Cu. As shown in Figure 3c, the catalytic activity of laccase decreased significantly as NaCl concentration increased. This decline is attributed to the high ionic strength, which influences the charge distribution, spatial structure, and solubility of the enzyme, resulting in a severe loss of catalytic activity. Intriguingly, HH-Cu displayed the opposite trend: its catalytic activity increased with rising NaCl concentration. Under the condition of 500 mM NaCl, the catalytic activity of HH-Cu was enhanced to approximately 285% of its original activity. This augmentation might be attributed to enhanced substrate binding efficiency to HH-Cu.[6]

Solvent influence of solvent on catalytic activity of laccase and HH-Cu was also probed by introducing varying ethanol concentrations (0, 25, 50, 70, and 100% v/v) into the reaction system. Figure 3d indicates that both HH-Cu and laccase

https://doi.org/10.1021/acsomega.5c00623
ACS Omega 2025, 10, 15553−15562

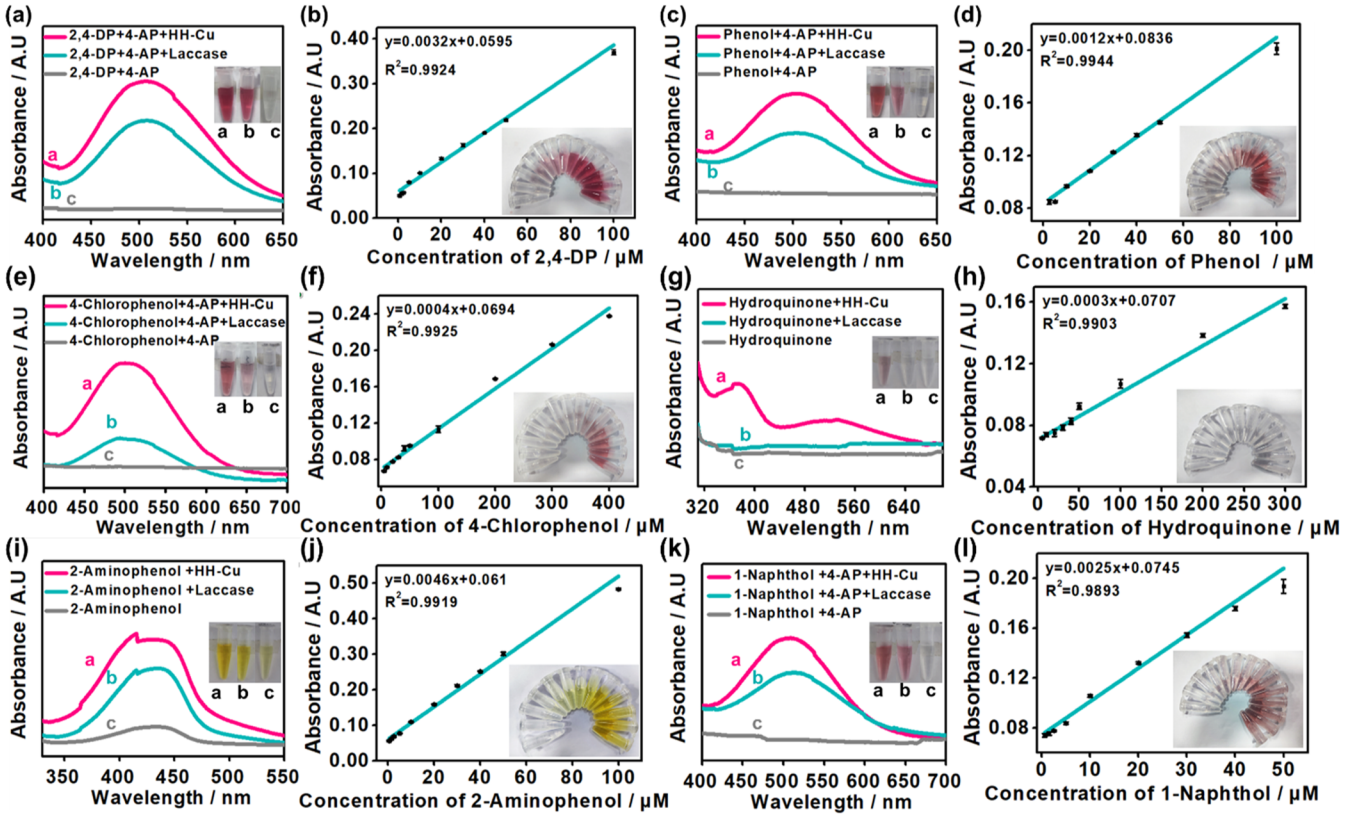

Figure 4. UV−vis spectrum of 2,4-DP (a), phenol (c), 4-chlorophenol (e), hydroquinone (g), 2-aminophenol (i), and 1-naphthol (k) catalyzed by HH-Cu and laccase. (b, d, f, h, j, l) The absorbance at the corresponding absorption maxima versus concentration of corresponding substrates catalyzed by HH-Cu. The insets are the corresponding photographs.

demonstrated reduced activity with higher ethanol content with a complete loss of activity at 50% ethanol. This result is consistent with the previous results showing that the catalytic activities of many laccase-mimicking nanozymes were significantly hindered by organic solvents.[6,8] We characterized the morphology of HH-Cu in 50% ethanol and confirmed that the nanoparticles maintained their original structure (Figure S9), ruling out structural degradation as the cause of the activity loss. Additionally, we bubbled oxygen into the reaction mixture and observed no catalytic activity from either HH-Cu or laccase, indicating that the absence of oxygen is not the limiting factor. This suggests that the ethanol solvent itself is responsible for hindering the reaction.

Furthermore, the storage stability of laccase and HH-Cu was assessed. They were kept at room temperature, and their catalytic activities were measured after 1, 2, 3, 5, 7, 9, and 11 days. Figure 3e illustrates a progressive decline in the catalytic activity of laccase, almost vanishing on the 9th day. In contrast, the catalytic activity of HH-Cu remained consistently stable, retaining over 90% of its original activity on the 12th day, showcasing its excellent storage stability.

To evaluate the recyclability of HH-Cu, we added 2,4-DP and 4-AP to MES buffer along with HH-Cu, and after reaction for 1 h, we collected HH-Cu by centrifugation, washed it with Milli-Q water, and reused it for subsequent cycles. As shown in Figure 3f, HH-Cu still retained 60% of its initial catalytic activity even after 10 cycles, while laccase could not be recycled. In conclusion, compared with laccase, HH-Cu exhibits excellent catalytic stability, storage stability, and recyclability.

3.3. Degradation and Determination of Phenolic Pollutants and Epinephrine. HH-Cu was exploited for degradation and detection of phenolic pollutants including 2,4-DP, phenol, 4-chlorophenol, hydroquinone, 2-aminophenol, and 1-naphthol. Some of these compounds underwent direct degradation to form colored oxidation products, such as hydroquinone and 2-aminophenol, enabling their quantification. For some phenolic compounds that did not form colored oxidation products, such as 2,4-DP, phenol, 4-chlorophenol, and 1-naphthol, we added the colorimetric reagent 4-AP, resulting in the formation of characteristic wine-red products with a maximum absorption at 510 nm, enabling the quantification of these compounds. At the same mass concentration, HH-Cu exhibited notably superior degradation efficiency for these phenolic pollutants compared to laccase (Figure 4a,c,e,g,i,k,). Figure 4 and Table 1 provide the detection limits and linear ranges for the respective substrates, demonstrating that HH-Cu can serve as a colorimetric sensor for phenolic pollutants.

Table 1. Detection Limit and Linear Range of HH-Cu for Different Phenolic Compounds

substrates	linear range (μM)	limit of detection
2,4-DP	0.6−100	442 nM
phenol	2.5−100	1.18 μM
4-chlorophenol	5−400	3.53 μM
hydroquinone	5−300	4.71 μM
2-aminophenol	0.5−100	307 nM
1-naphthol	0.6−50	565 nM

https://doi.org/10.1021/acsomega.5c00623
ACS Omega 2025, 10, 15553−15562

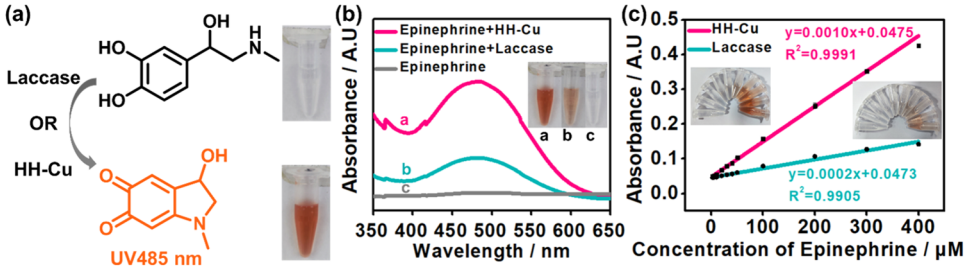

Figure 5. Comparison of the laccase-like activity of HH-Cu with laccase in catalyzing epinephrine. (a) Photographs of epinephrine and its oxidized product catalyzed by HH-Cu and laccase. (b) UV−vis spectrum of epinephrine catalyzed by HH-Cu and laccase. (c) The absorbance at 485 nm versus concentration of epinephrine catalyzed by HH-Cu and laccase. The insets in (b) and (c) are the corresponding photographs.

Furthermore, HH-Cu has been successfully employed as a colorimetric sensor for the detection of epinephrine. Both HH-Cu and laccase catalyzed the oxidation of epinephrine and produced orange-colored oxidation products with maximum absorption at 485 nm (Figure 5a). At the same mass concentration, HH-Cu exhibited substantially enhanced catalytic efficiency for epinephrine compared to laccase (Figure 5b). Different concentrations of epinephrine were catalyzed by HH-Cu and laccase (Figure 5c). The linear ranges for epinephrine detection using HH-Cu and laccase are 2−400 μM (R^2 = 0.9991) and 10−700 μM (R^2 = 0.9905), respectively. The detection limits were determined to be 1.41 and 7.07 μM for HH-Cu and laccase, respectively, indicating that HH-Cu provides higher sensitivity for epinephrine detection. Additionally, HH-Cu shows comparable detection limits for epinephrine and a wider linear range compared with the previously reported laccase mimics (Table 2). Additionally, to demonstrate the robustness and reproducibility of the HH-Cu, we have compared the catalytic activities of two separate batches of the synthesized material toward epinephrine. The results (Figure S10) indicate that the catalytic activities of both batches are virtually identical, which strongly supports the robustness and reproducibility of the HH-Cu system.

Table 2. Comparison of the Colorimetric Epinephrine Sensors Based on Laccase-like Activity

catalyst	linear range (μM)	limit of detection (μM)	reference
HH-Cu	2−400	1.41	this work
laccase	10−700	7.07	this work
AgCit	2.35−579.71	0.714	25
Cu/GMP	5−50	2.24	20
GNFs		1.64	41
Cu_2O nanospheres		10	43
Cu-tannic acid nanohybrids	4.5−90	3.4	44
CH-Cu	5−50	1.69	6
Fe_1@CN-20	27.3−273.2	1.30	8

4. CONCLUSIONS

The widespread application of laccase mimics has been severely hindered by their expensive and complicated synthesis routes. For example, researchers often use peptides to coordinate with copper ions to mimic the active sites of laccases, thereby constructing laccase mimics, but these synthetic methods are quite complicated, such as requiring high temperatures, using organic solvents, and cumbersome procedures. In this regard, we have demonstrated a simple yet highly active, robust, and functional laccase mimic HH-Cu. The synthesis of HH-Cu is based on a straightforward precipitation reaction by mixing the dipeptide HH and Cu^{2+} in PBS. By modulating the ratio of HH to copper ions, we obtained the best-performing organic−inorganic hybrid nanoparticles HH-Cu, which is superior to HH-Cu nanoflowers. Compared to natural enzymes, HH-Cu has 4.7-fold higher v_{max} and lower K_m and is robust under harsh conditions, including high temperature, extreme pH, and high ionic strength. Furthermore, HH-Cu showed excellent storage stability and reusability. Our research has successfully harnessed HH-Cu for the degradation and detection of a spectrum of phenolic compounds, including 2,4-DP, phenol, 4-chlorophenol, hydroquinone, 2-aminophenol, 1-naphthol, and epinephrine. Notably, in the detection of epinephrine, HH-Cu outperformed laccase with a notably lower detection limit (1.41 μM compared to 7.07 μM). In summary, our laccase mimic HH-Cu not only demonstrates superior catalytic performance and robustness under harsh conditions but also offers a simple and cost-effective synthesis route, making it highly promising for practical applications in environmental remediation and biosensing.

■ ASSOCIATED CONTENT

Supporting Information

The Supporting Information is available free of charge at https://pubs.acs.org/doi/10.1021/acsomega.5c00623.

Figure S1: comparison of catalytic activity between precipitate and supernatant of dispersed HH-Cu solution; Figure S2: SEM images of HH-2Cu and HH-3Cu; Figure S3: full-scan XPS spectra of HH-Cu and HH-2Cu; Figure S4: Cu 2p XPS spectrum of HH-2Cu; Figure S5: SEM images of control groups $Cu_3(PO_4)_2$ and HH; Figure S6: Michaelis−Menten and Lineweaver−Burk plots for HH-Cu and laccase; Table S1: kinetic parameters of 2,4-DP and 4-AP reactions catalyzed by HH-Cu, laccase, and laccase mimics; Figure S7: SEM images of HH-Cu incubated at various pH values; Figure S8: SEM images of HH-Cu incubated at various temperatures (PDF)

■ AUTHOR INFORMATION

Corresponding Authors

Yongfang Zheng − *Fujian−Taiwan Science and Technology Cooperation Base of Biomedical Materials and Tissue Engineering, Engineering Research Center of Industrial Biocatalysis, Fujian Provincial Key Laboratory of Polymer*

https://doi.org/10.1021/acsomega.5c00623
ACS Omega 2025, 10, 15553−15562

Materials, College of Chemistry and Materials Science, Fujian Normal University, Fuzhou 350007, China; orcid.org/0000-0002-6650-0599; Email: zhengyf20@fjnu.edu.cn

Hu Zhu − *Fujian−Taiwan Science and Technology Cooperation Base of Biomedical Materials and Tissue Engineering, Engineering Research Center of Industrial Biocatalysis, Fujian Provincial Key Laboratory of Polymer Materials, College of Chemistry and Materials Science, Fujian Normal University, Fuzhou 350007, China; Key Laboratory of Translational Tumor Medicine in Fujian Province, Putian University, Putian 351100, China;* orcid.org/0000-0002-8359-3758; Email: zhuhu@fjnu.edu.cn

Authors

Lisha Feng − *Fujian−Taiwan Science and Technology Cooperation Base of Biomedical Materials and Tissue Engineering, Engineering Research Center of Industrial Biocatalysis, Fujian Provincial Key Laboratory of Polymer Materials, College of Chemistry and Materials Science, Fujian Normal University, Fuzhou 350007, China*

Kejing Mao − *Fujian−Taiwan Science and Technology Cooperation Base of Biomedical Materials and Tissue Engineering, Engineering Research Center of Industrial Biocatalysis, Fujian Provincial Key Laboratory of Polymer Materials, College of Chemistry and Materials Science, Fujian Normal University, Fuzhou 350007, China*

Xinyu Zhu − *Fujian−Taiwan Science and Technology Cooperation Base of Biomedical Materials and Tissue Engineering, Engineering Research Center of Industrial Biocatalysis, Fujian Provincial Key Laboratory of Polymer Materials, College of Chemistry and Materials Science, Fujian Normal University, Fuzhou 350007, China*

Yuyuan Chen − *Fujian−Taiwan Science and Technology Cooperation Base of Biomedical Materials and Tissue Engineering, Engineering Research Center of Industrial Biocatalysis, Fujian Provincial Key Laboratory of Polymer Materials, College of Chemistry and Materials Science, Fujian Normal University, Fuzhou 350007, China*

Jianbin Ye − *Key Laboratory of Translational Tumor Medicine in Fujian Province, Putian University, Putian 351100, China*

Complete contact information is available at: https://pubs.acs.org/10.1021/acsomega.5c00623

Notes

The authors declare no competing financial interest.

■ ACKNOWLEDGMENTS

This work was financially supported by the Natural Science Foundation of China (22307018 and U1805234), the Natural Science Foundation of Fujian Province of China (2021J05033 and 2023H6011), Program for Innovative Research Team in Science and Technology in Fujian Province University, 100 Talents Program of Fujian Province, Fujian-Taiwan Science and Technology Cooperation Base of Biomedical Materials and Tissue Engineering (2021D039), Fu-Xia-Quan National Independent Innovation Demonstration Zone Collaborative Innovation Platform Project (2022FX3), Major Scientific Research Program for Young and Middle-aged Health Professionals of Fujian Province, China (2023ZQNZD020), and Scientific Research Start-up Fund for High-Level Talents in Fujian Normal University.

■ REFERENCES

(1) Rao, M. L.; Strebel, B.; Halaris, A.; Gross, G.; Braunig, P.; Huber, G.; Marler, M. Circadian rhythm of vital signs, norepinephrine, epinephrine, thyroid hormones, and cortisol in schizophrenia. *Psychiatry Res.* **1995**, *57*, 21−39.

(2) Barcroft, H.; Peterson, E.; Schwab, R. S. Action of adrenaline and noradrenaline on the tremor in Parkinson's disease. *Neurology* **1952**, *2*, 154−160.

(3) Wichit, P.; Thanprasertsuk, S.; Hopetrungraung, T.; Phokaewvarangkul, O.; Bongsebandhu-phubhakdi, S.; Bhidayasiri, R. Increased epinephrine in the saliva of Parkinson's disease patients: A preliminary observation. *Movement Disord.* **2020**, *35*, 372−373.

(4) Burke, W. J.; Li, S. W.; Chung, H. D.; Ruggiero, D. A.; Kristal, B. S.; Johnson, E. M.; Lampe, P.; Kumar, V. B.; Franko, M.; Williams, E. A.; Zahm, D. S. Neurotoxicity of MAO metabolites of catecholamine neurotransmitters: Role in neurodegenerative diseases. *Neurotoxicology* **2004**, *25*, 101−115.

(5) Pérez-Jiménez, J.; Torres, J. L. Analysis of Nonextractable Phenolic Compounds in Foods: The Current State of the Art. *J. Agric. Food Chem.* **2011**, *59*, 12713−12724.

(6) Wang, J.; Huang, R.; Qi, W.; Su, R.; Binks, B. P.; He, Z. Construction of a bioinspired laccase-mimicking nanozyme for the degradation and detection of phenolic pollutants. *Appl. Catal., B* **2019**, *254*, 452−462.

(7) Li, M.; Xie, Y.; Song, D.; Huang, H.; Li, Y. 2-Methylimidazole-doped nanozymes with enhanced laccase activity for the (+)-catechins detection in dairy products. *Talanta* **2023**, *252*, No. 123853.

(8) Lin, Y. M.; Wang, F.; Yu, J.; Zhang, X.; Lu, G. P. Iron single-atom anchored N-doped carbon as a 'laccase-like' nanozyme for the degradation and detection of phenolic pollutants and adrenaline. *J. Hazard. Mater.* **2022**, *425*, No. 127763.

(9) de Oliveira Neto, J. R.; Rezende, S. G.; Lobon, G. S.; Garcia, T. A.; Lopes Macedo, I. Y.; Garcia, L. F.; Alves, V. F.; Sapateiro Torres, I. M.; Santiago, M. F.; Schmidt, F.; Gil, E. S. Electroanalysis and laccase-based biosensor on the determination of phenolic content and antioxidant power of honey samples. *Food Chem.* **2017**, *237*, 1118−1123.

(10) Tang, C.; Guo, T.; Zhang, Z.; Yang, P.; Song, H. Rapid visualized characterization of phenolic taste compounds in tea extract by high-performance thin-layer chromatography coupled to desorption electrospray ionization mass spectrometry. *Food Chem.* **2021**, *355*, No. 129555.

(11) Rodríguez-Delgado, M. M.; Aleman-Nava, G. S.; Rodriguez-Delgado, J. Manuel.; Dieck-Assad, G.; Martinez-Chapa, S. O.; Barcelo, D.; Parra, R. Laccase-based biosensors for detection of phenolic compounds. *TrAC, Trends Anal. Chem.* **2015**, *74*, 21−45.

(12) Ye, M.-L.; Zhu, Y.; Lu, Y.; Gan, L.; Zhang, Y.; Zhao, Y.-G. Magnetic nanomaterials with unique nanozymes-like characteristics for colorimetric sensors: A review. *Talanta* **2021**, *230*, No. 122299.

(13) Datta, S.; Veena, R.; Samuel, M. S.; Selvarajan, E. Immobilization of laccases and applications for the detection and remediation of pollutants: a review. *Environ. Chem. Lett.* **2021**, *19*, 521−538.

(14) Gao, L.; Zhuang, J.; Nie, L.; Zhang, J.; Zhang, Y.; Gu, N.; Wang, T.; Feng, J.; Yang, D.; Perrett, S.; Yan, X. Intrinsic peroxidase-like activity of ferromagnetic nanoparticles. *Nat. Nanotechnol.* **2007**, *2*, 577−583.

(15) Wei, H.; Gao, L.; Fan, K.; Liu, J.; He, J.; Qu, X.; Dong, S.; Wang, E.; Yan, X. Nanozymes: A clear definition with fuzzy edges. *Nano Today* **2021**, *40*, No. 101269.

(16) Wu, J.; Wang, X.; Wang, Q.; Lou, Z.; Li, S.; Zhu, Y.; Qin, L.; Wei, H. Nanomaterials with enzyme-like characteristics (nanozymes): next-generation artificial enzymes (II). *Chem. Soc. Rev.* **2019**, *48*, 1004−1076.

(17) Huang, Y.; Ren, J.; Qu, X. Nanozymes: Classification, Catalytic Mechanisms, Activity Regulation, and Applications. *Chem. Rev.* **2019**, *119*, 4357−4412.

(18) Tian, L.; Qi, L.; Liu, Y. T.; Zhao, Z. W.; Liu, W. Boosting the LAC-like activity of tetrapeptide capped copper nanoparticle-based

nanozymes for colorimetric determination of adrenaline. *Anal. Methods* **2024**, *16*, 1383−1389.
(19) Chai, T.-Q.; Wang, J.-L.; Chen, G.-Y.; Chen, L.-X.; Yang, F.-Q. Tris-Copper Nanozyme as a Novel Laccase Mimic for the Detection and Degradation of Phenolic Compounds. *Sensors* **2023**, *23*, No. 8137, DOI: 10.3390/s23198137.
(20) Liang, H.; Lin, F.; Zhang, Z.; Liu, B.; Jiang, S.; Yuan, Q.; Liu, J. Multicopper Laccase Mimicking Nanozymes with Nucleotides as Ligands. *ACS Appl. Mater. Interfaces* **2017**, *9*, 1352−1360.
(21) Yang, Y.; Xu, J.; Guo, Y.; Wang, X.; Xiao, L.-P.; Zhou, J. Biodegradation of Lignin into Low-Molecular-Weight Oligomers by Multicopper Laccase-Mimicking Nanozymes of the Cu/GMP Complex at Room Temperature. *ACS Sustainable Chem. Eng.* **2022**, *10*, 5489−5499.
(22) Li, X.; Zhang, Y.; Tan, W.; Jin, P.; Zhang, P.; Li, K. Bioinspired Coassembly of Copper Ions and Nicotinamide Adenine Dinucleotides for Single-Site Nanozyme with Dual Catalytic Functions. *Anal. Chem.* **2023**, *95*, 2865−2873.
(23) Yan, X.; Li, H.; Wang, T.; Li, A.; Zhu, C.; Lu, G. Engineering of coordination environment in bioinspired laccase-mimicking catalysts for monitoring of pesticide poisoning. *Chem. Eng. J.* **2022**, *446*, No. 136930.
(24) Li, A. X.; Li, H. X.; Ma, Y.; Wang, T. H.; Liu, X. M.; Wang, C. G.; Liu, F. M.; Sun, P.; Yan, X.; Lu, G. Y. Bioinspired laccase-mimicking catalyst for on-site monitoring of thiram in paper-based colorimetric platform. *Biosens. Bioelectron.* **2022**, *207*, No. 114199.
(25) Koyappayil, A.; Kim, H. T.; Lee, M.-H. Laccase-like properties of coral-like silver citrate micro-structures for the degradation and determination of phenolic pollutants and adrenaline. *J. Hazard. Mater.* **2021**, *412*, No. 125211.
(26) Liang, S.; Wu, X.-L.; Xiong, J.; Yuan, X.; Liu, S.-L.; Zong, M.-H.; Lou, W.-Y. Multivalent Ce-MOFs as biomimetic laccase nanozyme for environmental remediation. *Chem. Eng. J.* **2022**, *450*, No. 138220.
(27) Huang, L.; Tang, Y.; Wang, J.; Niu, X.; Zhou, J.; Wu, Y. Cubic Ag2O nanoparticles as robust laccase mimetics in a smartphone-assisted colorimetric sensor for rapid and ultrasensitive detection of kanamycin in environment. *Sens. Actuators, B* **2023**, *391*, No. 134052.
(28) Tang, Q.; Zhou, C.; Shi, L.; Zhu, X.; Liu, W.; Li, B.; Jin, Y. Multifunctional Manganese-Nucleotide Laccase-Mimicking Nanozyme for Degradation of Organic Pollutants and Visual Assay of Epinephrine via Smartphone. *Anal. Chem.* **2024**, *96*, 4736−4744.
(29) Xu, X.; Wang, J.; Huang, R.; Qi, W.; Su, R.; He, Z. Preparation of laccase mimicking nanozymes and their catalytic oxidation of phenolic pollutants. *Catal. Sci. Technol.* **2021**, *11*, 3402−3410.
(30) Ge, J.; Lei, J.; Zare, R. N. Protein-inorganic hybrid nanoflowers. *Nat. Nanotechnol.* **2012**, *7*, 428−432.
(31) Jafari-Nodoushan, H.; Mojtabavi, S.; Faramarzi, M. A.; Samadi, N. Organic-inorganic hybrid nanoflowers: The known, the unknown, and the future. *Adv. Colloid Interface Sci.* **2022**, *309*, No. 102780.
(32) Wei, T.; Du, D.; Zhu, M.-J.; Lin, Y.; Dai, Z. An Improved Ultrasensitive Enzyme-Linked Immunosorbent Assay Using Hydrangea-Like Antibody-Enzyme-Inorganic Three-in-One Nanocomposites. *ACS Appl. Mater. Interfaces* **2016**, *8*, 11892.
(33) Dega, N. K.; Ganganboina, A. B.; Tran, H. L.; Kuncoro, E. P.; Doong, R.-a. BSA-stabilized manganese phosphate nanoflower with enhanced nanozyme activity for highly sensitive and rapid detection of glutathione. *Talanta* **2022**, *237*, No. 122957.
(34) Ye, R.; Zhu, C.; Song, Y.; Lu, Q.; Ge, X.; Yang, X.; Zhu, M.-J.; Du, D.; Li, H.; Lin, Y. Bioinspired Synthesis of All-in-One Organic-Inorganic Hybrid Nanoflowers Combined with a Handheld pH Meter for On-Site Detection of Food Pathogen. *Small* **2016**, *12*, 3094−3100.
(35) Mostafavi, M.; Mahmoodzadeh, K.; Habibi, Z.; Yousefi, M.; Brask, J.; Mohammadi, M. Immobilization of Bacillus amyloliquefaciens protease ?Neutrase? as hybrid enzyme inorganic nanoflower particles: A new biocatalyst for aldol-type and multicomponent reactions. *Int. J. Biol. Macromol.* **2023**, *230*, No. 123140.
(36) Rong, J.; Zhang, T.; Qiu, F.; Zhu, Y. Preparation of Efficient, Stable, and Reusable Laccase-Cu-3(PO4)(2) Hybrid Microspheres Based on Copper Foil for Decoloration of Congo Red. *ACS Sustainable Chem. Eng.* **2017**, *5*, 4468−4477.
(37) Han, Z.; Wang, H.; Zheng, J.; Wang, S.; Yu, S.; Lu, L. Ultrafast synthesis of laccase-copper phosphate hybrid nanoflowers for efficient degradation of tetracycline antibiotics. *Environ. Res.* **2023**, *216*, No. 114690.
(38) Luo, M.; Li, M.; Jiang, S.; Shao, H.; Razal, J.; Wang, D.; Fang, J. Supported growth of inorganic-organic nanoflowers on 3D hierarchically porous nanofibrous membrane for enhanced enzymatic water treatment. *J. Hazard. Mater.* **2020**, *381*, No. 120947.
(39) Guo, J.; Wang, Y.; Zhao, M. A self-activated nanobiocatalytic cascade system based on an enzyme-inorganic hybrid nanoflower for colorimetric and visual detection of glucose in human serum. *Sens. Actuators, B* **2019**, *284*, 45−54.
(40) Cheon, H. J.; Adhikari, M. D.; Chung, M.; Tran, T. D.; Kim, J.; Kim, M. I. Magnetic Nanoparticles-Embedded Enzyme-Inorganic Hybrid Nanoflowers with Enhanced Peroxidase-Like Activity and Substrate Channeling for Glucose Biosensing. *Adv. Healthcare Mater.* **2019**, *8*, No. 1801507.
(41) Tran, T. D.; Nguyen, P. T.; Le, T. N.; Kim, M. I. DNA-copper hybrid nanoflowers as efficient laccase mimics for colorimetric detection of phenolic compounds in paper microfluidic devices. *Biosens. Bioelectron.* **2021**, *182*, No. 113187.
(42) Xia, L.; Huang, A.; Niu, X.; Wu, Z.; Tang, Y.; Zhou, J.; Wu, Y. Laccase-mimicking activity of octahedral Mn3O4 nanoparticles and fluorescence of carbon dots as dual-mode signals for the specific detection of arsenic(V) in environmental water samples. *Sci. Total Environ.* **2024**, *951*, No. 175559.
(43) Maity, T.; Jain, S.; Solra, M.; Barman, S.; Rana, S. Robust and Reusable Laccase Mimetic Copper Oxide Nanozyme for Phenolic Oxidation and Biosensing. *ACS Sustainable Chem. Eng.* **2022**, *10*, 1398−1407.
(44) Ma, H.; Zheng, N.; Chen, Y.; Jiang, L. Laccase-like catalytic activity of Cu-tannic acid nanohybrids and their application for epinephrine detection. *Colloids Surf., A* **2021**, *613*, No. 126105.

https://doi.org/10.1021/acsomega.5c00623
ACS Omega 2025, 10, 15553−15562